Xiaofeng Zhang, Venu Mahesh, David Ng, Ryan Hubbard, Amit Ailiani, Bernie O'Hare, Alan Benesi and Andrew Webb.

Design, construction and NMR testing of a 1 tesla Halbach Permanent Magnet for Magnetic Resonance

Abstract Widespread use of magnetic resonance imaging (MRI) and nuclear magnetic resonance (NMR) spectroscopy in research, industry, and education is limited by the physical size and the very high procurement and maintainance costs of a superconducting magnet. Attempts have been made to replace the superconducting magnet with a permanent magnet. However, the reported permanent magnets have typically been limited to very low field strengths, or very small useable volumes. In this paper, we introduce a design of a portable table-top magnet with a field strength of 1 tesla (i.e., a ^1H resonance frequency of 42.5 MHz), which consists of an array of 36 cylindrical permanent magnet rods positioned to achieve a reasonably homogeneous magnetic field within an extended region. Three-dimensional (3D) numerical magnetostatic simulations were performed using FEMLAB. The simulated results of the magnetic flux density, frequently referred to as the "B_0 field" in the MRI and NMR community, were compared with the measurements obtained using a digital teslameter. The simulated and measured B_0 field were found to be very similar. The initial utility of the permanent magnet has been demonstrated by the acquisition of NMR spectra using a custom-built microcoil probe.

Finally, FEMLAB simulations were performed to determine an improved topological design to increase the strength of the B_0 field using existing magnets.

Keywords permanent magnet, miniature, magnetic resonance, imaging, spectroscopy, simulation, FEMLAB

1 Introduction

Magnetic resonance imaging (MRI) and nuclear magnetic resonance (NMR) have found widespread applications in a variety of fields. However, the physical size and the high procurement and maintainance costs of a superconducting magnet are frequently prohibitive for many important applications, such as on-site diagnosis, integrated chemical analysis, and education.

A promising alternative technology is to replace the superconducting magnet with a permanet magnet. This technology has become feasible with the availability of new magnetic materials [1,2]. However, the reported strength of magnetic field B_0 are typically inadequate for practical applications.

2 Design and Construction

In this paper, we describe a portable table-top Halbach [3,4] magnet with a field strength greater than 1 tesla (i.e., a ^1H resonance frequency higher than 42.5 MHz), which is adequate for "low-field" magnetic resonance applications.

The principle of the Halbach magnet was proposed by Klaus Halbach for particle accelerators [5]. It removes the requirement for a large magnetic conductor (i.e., the "yoke") by positioning permanent magnet elements in such a way that magnetic fields interfere destructively with each other in certain regions, while interfering constructively in others. The design strategy for our magnet array is as follows: utilizing the reciprocity between the external and the internal magnetic fields, an "internal" magnetic field is generated in free space by aligning the magnetic flux lines of the magnet elements with those of the "external" field. This creates a usable volume of B_0 field for MRI and MRS applications.

Without an iron yoke, not only can the weight and volume of the magnet be reduced significantly, but more importantly the limitation to the maximum field strength, as a result of magnetic saturation of magnetic conductors (for magnets made from SmCo and NdFeB in particular), can be circumvented. Another advantage of the Halbach design is that it makes possible creating a much higher field strength than any individual magnet element, which is limited by the remanence (currently 1.35 T with AlNiCo magnet) and demagnetization of the magnetic material (currently ~2 T) because the core field does not pass through the magnet elements. For this

Prof. Andrew Webb
Department of Bioengineering
Pennsylvania State University
315 Hallowell Building
State College, PA 16802
Tel: (814) 865-0459
Fax: (814) 863-0490
E-mail: agw@engr.psu.edu

reason, according to Abele et al. [6], the upper limit of the core magnetic field can therefore be extended to 5 T before demagnetization occurs.

In summary, the Halbach array has the following advantages: the strength of the core field can exceed the limitation imposed by material demagnetization, yokeless design effectively miniaturizes the magnet and eliminates considerations of magnetic saturation, and fields from magnet elements add linearly although they decrease in magnitude as a function of r^{-2} as the elements are positioned farther away from the center.

Our permanent magnet (16 × 23 mm clear bore size, 38 lb. weight) consists of an array of 36 cylindrical permanent magnet elements (NdFeB, diameter 20 mm, length 150 mm, 60541 magnet, China Rare Earth Magnet, Shen Zhen, China) positioned hexagonally in two layers. The magnet elements were characterized using a digital teslameter and paired for optimum homogeneity. Each pair was then aligned according to its magnetic field polarity and fixed into an aluminum tube using epoxy. The rods were then positioned and oriented as shown in Figure 1. Special effort was taken to maintain high mechanical precision during construction.

3 Numerical Simulations

Three-dimensional (3D) magnetostatic numerical simulations were performed using FEMLAB (version 3.1, COMSOL, Stockholm, Sweden). The exact value of the magnetization for each magnet element was determined by setting the value of the simulated magnetic flux density on the surface of an individual element to that measured using a teslameter. The 2-D map of the y-component of the simulated magnetic flux density, i.e., the B_0 field, is shown in Fig. 2(a), which has reasonably good homogeneity within the magnet bore for a prototype. Figs. 2(b) and 2(c) show the 1-D profiles of this map along the x- and the y-axes, respectively.

The profiles of the simulated B_0 field along the longitudinal axis (i.e., the z-axis) of the magnet at two different locations along the y-axis (at the center and the side of the magnet bore, respectively) were compared with measurements (Figure 3). The two results were consistent with each other except for a relatively small difference in their absolute values. This difference was likely caused by error in determining the measurement position, as a result of the relatively large size of the detector of the teslameter compared with the size of the permanent magnet elements.
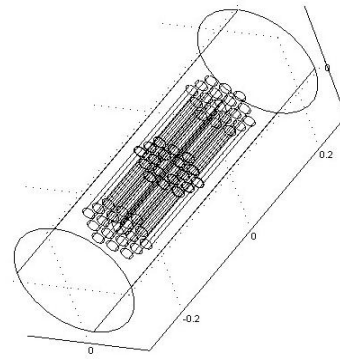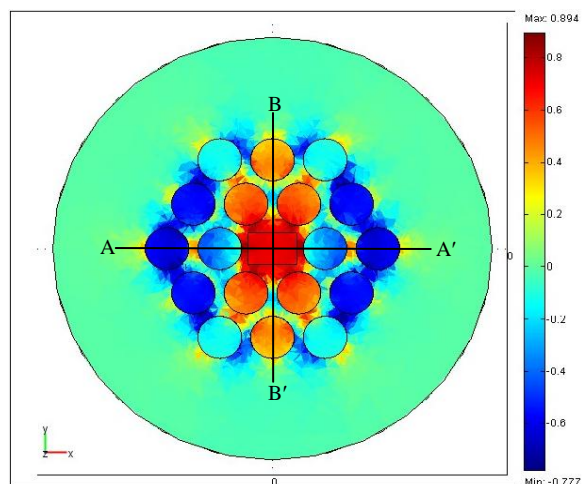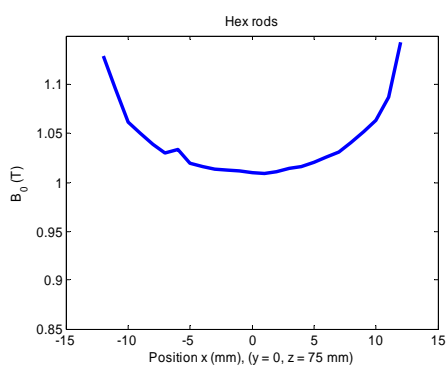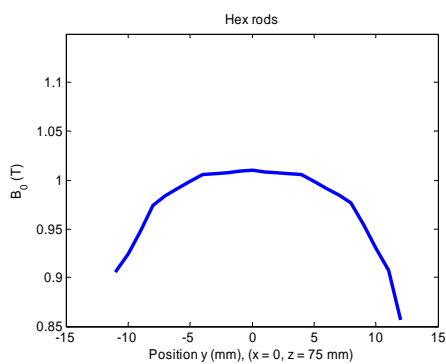

(a)
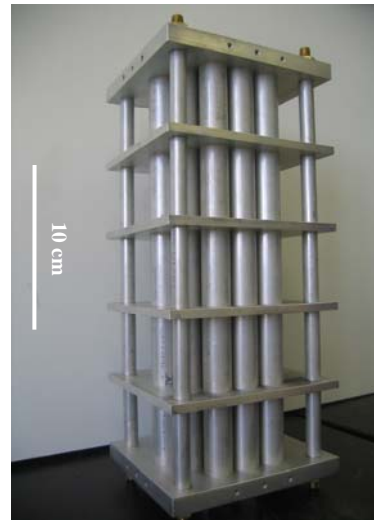
(b)
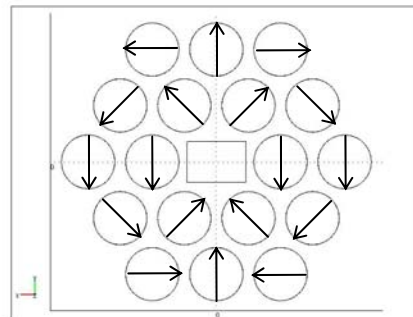
(c)

Figure 1. (a) Schematic and (b) photograph of the permanent magnet. (c) Orientations of each magnet element, shown as an arrow, with the rectangle in the center representing the useable magnet bore.

(a)

(b)

(c)

Figure 2. (a) Simulated magnetic flux density (B_0 field) from the central plane of the permanent magnet. Profile along (b) A-A′ (i.e., the x-axis) and B-B′ (i.e., the y-axis).

4 NMR Experiments

The radio-frequency (RF) probe (Fig. 4) used for the NMR experiments was a solenoid (54 turns compact windding, 10 mm length) made of polyimide-clad copper wire (30 AWG), wound on a polyimide sheath (1.2 mm o.d., 1.0 mm i.d.), and tuned to 44.3 MHz (B_0 field 1.04 T). A glass capillary
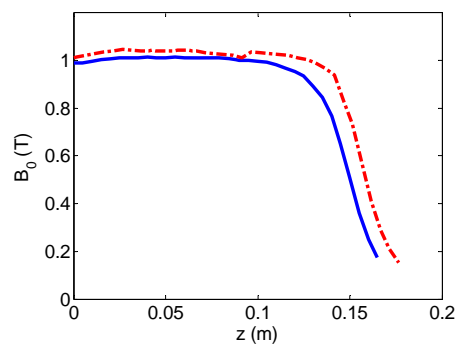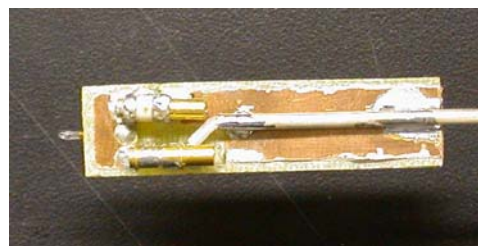

(a)
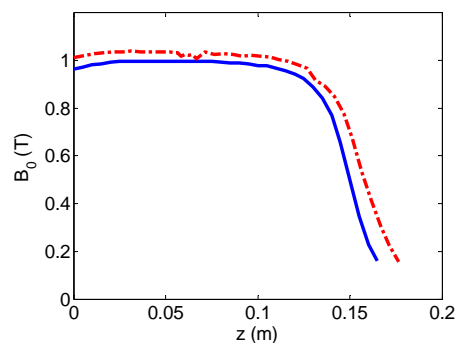
(b)

Figure 3. Comparison of the simulated (blue) and the measured (red) magnetic flux density B_0 along the longitudinal axis at: (a) the center and (b) the inner surface of the bore of the magnet.

(a)

(b)

Figure 4. The NMR probe: (a) the solenoid with sample inside, and (b) the circuit board with variable impedance matching capacitors.

tube (1.0 mm o.d., 0.8 mm i.d.) can be slid into the sheath allowing easy sample changing. The sample

used in these first experiments was pure water. The loaded probe has a Q value of 56 and a tuning range of 40.5-45.5 MHz. A spin-echo sequence, with a 16-step phase cycle, was used to acquire the NMR signal: the echo time (TE) was 60 μs. The 90-degree pulse width was 1 μs at a power of approximately 25 W. Figure 5(a) shows the echo amplitude as a function of pulse length between 0.2 and 3.2 μs; Figure 5(b) shows the time-domain echo signal; and Figure 5(c) is the corresponding frequency spectrum. The linewidth of the spectrum was approximately 100 kHz.
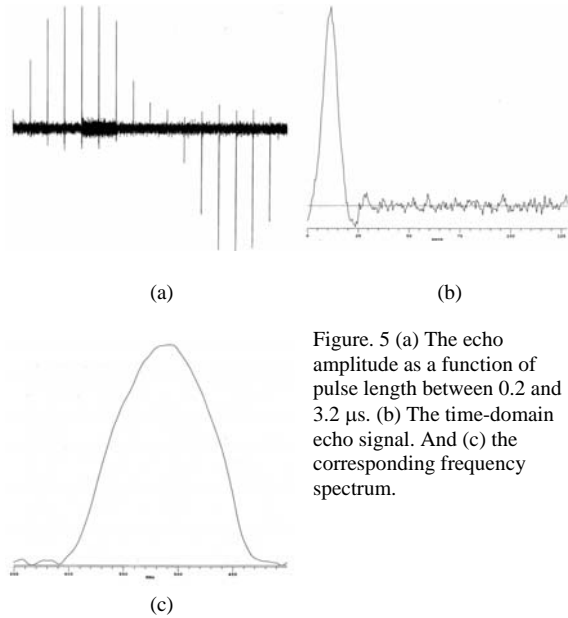

(a)   (b)

Figure. 5 (a) The echo amplitude as a function of pulse length between 0.2 and 3.2 μs. (b) The time-domain echo signal. And (c) the corresponding frequency spectrum.

(c)

5 Simulations of Improved Magnet Geometries

As mentioned previously, the field strength of magnet elements add linearly. Two topologies were studied using simulations to investigate the effect of (a) individual element positioning and (b) changing the size of the magnet elements, on the strength of the overall field.

The two new designs were compared with a standard single-layer design, shown in Figure 6(a), which consists of small rectangular magnets (18 × 18 × 27 mm). By stacking four such layers together, we have experimentally constructed a permanent magnet with a field strength of 0.64 T and a bore-size of 20 × 20 mm (details of its structure and simulation results are not shown). Figure 6(b) illustrates an improved design, which utilizes two orthogonal layers of magnet elements to approximate a thick-walled spherical shell. The simulated field strength was increased by 40% using the design shown in Figure

6(b) compared with that of the design shown in Figure 6(a). Based on this design, the size of the magnet elements were increased (doubling its size in one or two dimensions whenever possible), as shown in Fig. 6 (c). The design shown in Figure 6(c) provided an overall improvement of 100%. A comparison of the profiles of the B_0 field along the x-axis (perpendicular to the B_0 field) for the above three designs are shown in Figure 7.
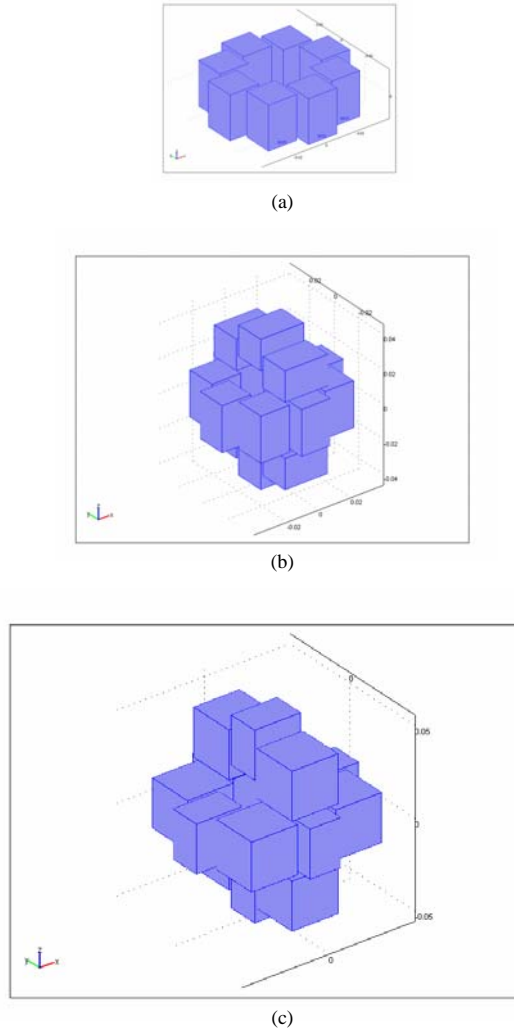

(a)

(b)

(c)

Figure 6. Designs of different arrangement and geometry of magnet elements (drawn to scale): (a) single-layer, (b) orthogonal layers, and (c) orthogonal layers using expended elements.

Further improvement of field strength and homogeneity is achievable by better approximating a spherical structure, an approach which we are still investigating.
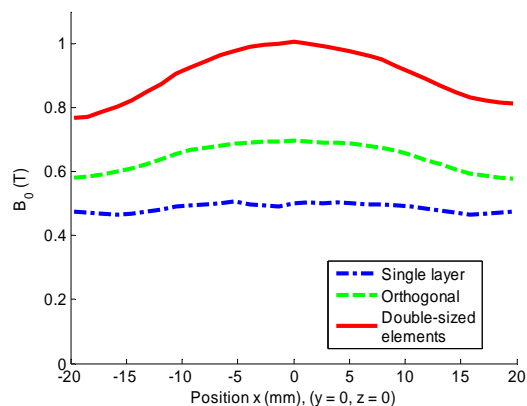
Figure 7. Profile of the B_0 field along the x-axis of the magnet for different designs: single-layer (blue dash line), orthogonal layers (green dot-dash line), and orthogonal layers using expended elements (red solid line). Horizontal axis: distance from the center of the magnet (mm); vertical axis : values of the simulated B_0 field (T).

6 Conclusions

A permanent magnet of a field strength of 1 T has been designed and constructed, and preliminary NMR data have been acquired to demonstrate its utility. With improved topological design, the field strength might be extended to above 2 T, which makes the miniature magnet attractive to potential MRI and MRS users.

References
1. R. Skomski, J.M.D. Coey, Permanent Magnetism, Philadelphia: Institute of Physics Publishing (1999)
2. R.J. Parker, Advances in Permanent Magnetism, New York: John Wiley & Sons (1990)
3. G. Moresi and R. Magin, Miniature Permanent Magnet for Table-top NMR, Concepts. Magn. Reson. B, 19B: 35-43 (2003)
4. H. Raich and P. Blumler, Design and Construction of a Dipolar Halbach Array with a Homogeneous Field from Identical Bar Magnets: NMR Mandhalas, Concepts. Magn. Reson. B, 23B: 16-25 (2004)
5. K. Halbach, Design of Permanent Multipole Magnets with Oriented Rare Earth Cobalt Materials, Nucl. Instr. Meth., 169: 1-10 (1980)
6. M. G. Abele, H.A. Leupold, and E. Potenziani, Applications of Yokeless Flux Confinement, J. App. Phy., 64(10): 5994-5996 (1988)